Characterization of soft stripe-domain deformations in Sm-*C* and Sm-*C** liquid-crystal elastomers

J. S. Biggins
Cavendish Laboratory, University of Cambridge, Madingley Road, Cambridge CB3 OHE, U.K.

K. Bhattacharya
Division of Engineering and Applied Science, Mail Code 104-44,California Institute of Technology, Pasadena CA 91125, USA

(Received 19 December 2008; revised manuscript received 20 March 2009; published 23 June 2009)

The neoclassical model of Sm-*C* (and Sm-*C**) elastomers developed by Warner and Adams predicts a class of "soft" (zero energy) deformations. We find and describe the full set of stripe domains—laminate structures in which the laminates alternate between two different deformations—that can form between pairs of these soft deformations. All the stripe domains fall into two classes, one in which the smectic layers are not bent at the interfaces, but for which—in the Sm-*C** case—the interfaces are charged, and one in which the smectic layers are bent but the interfaces are never charged. Striped deformations significantly enhance the softness of the macroscopic elastic response.

DOI: 10.1103/PhysRevE.79.061705 PACS number(s): 61.30.Vx, 83.80.Va, 62.20.D−, 61.41.+e

I. INTRODUCTION

Liquid-crystal elastomers [1] are cross-linked polymer networks (elastomers) with liquid-crystal phases embedded inside them. The liquid-crystal rods are chemically incorporated into the elastomer either as a simple component of the polymer chains or as pendent like side chains. Below a critical temperature, these rods align to form a liquid-crystal phase inside the elastomer. Any of the different liquid-crystal phases can be produced by tuning the temperature and composition of the elastomer, including a Sm-*C* phase in which, in addition to an average alignment, the liquid-crystal rods are also confined to layers and the layer normal is not parallel with the alignment. A schematic diagram of a Sm-*C* elastomer is shown in Fig. 1. If the liquid-crystal rods all have the same chirality (Sm-*C** as apposed to Sm-*C*), the system will also have a polarization along the cross product of the layer normal and the liquid-crystal director, that is, in the *y* direction.

Liquid-crystal elastomers show remarkable elastic properties because the polymer conformations are biased along the liquid-crystal director. This means the rotation of the director (and therefore of the bias) relative to the polymer network causes macroscopic shape changes in the elastomer at little energetic cost [2], generating soft (zero energy) modes of deformation. In a Sm-*C* elastomer, there are energy penalties associated with changing the layer spacing and the tilt angle. Therefore, the soft modes are those obtained by rotating the director in a cone around the layer normal [3].

If a nonsoft deformation is applied to a Sm-*C* elastomer, it may still be able to reduce its energy by splitting into small regions each of which undergoes a soft deformation such that the total deformation matches the imposed deformation. The stripe domains observed in nematic elastomers [4] are an example of this type of behavior. Such textures significantly enhance the macroscopic soft response of a material. This poses two interesting problems: what is the energy function of the material after the most favorable textures have been adopted, and what deformation patterns (textures) can form?

In this paper, we build on the work of Adams and Warner [3,5] to address the second question above. Specifically, we show that Sm-*C* has great freedom in forming stripe domains and characterize all possible stripe-domain textures and their morphology. By stripe domains, we mean alternating plates of two distinct director orientations and corresponding soft deformations separated by unbroken interfaces. Since every interface in a stripe domain is the same, one has only to examine a single interface which we do using tools developed to study twins in crystalline solids showing martensitic transitions. We note that the first question was addressed by Adams *et al.* [6].

Stripe-domain textures could be observed experimentally by imposing simple nonsoft deformations on Sm-*C* monodomain samples. Although the formation of more complicated higher-order textures (double and triple laminates) can be energetically favorable [6], these, as in nematic elastomers, are associated with deformations that stretch the sample in all directions perpendicular to the initial director. Since existing fabrication techniques produce thin films with the director in plane, such deformations cannot be imposed globally. Therefore, we anticipate that the observed textures will predominantly be stripe domains of the forms described in this paper.

This paper is organized as follows. We give a physical description of our results in Sec. II. We recall the theory of Adams and Warner and characterize the soft modes in the next section. In doing so, we make a different choice of reference configuration: one which is commonly used elsewhere [7] and one which makes further calculations simpler. We discuss the continuity of displacement across interfaces in Sec. V, characterize all stripe domains in Sec. VI, and examine ferroelectric properties in Sec. VII.

II. RESULTS

The soft deformations in Sm-*C* elastomers are caused by a rotation of the director relative to the underlying polymer network while leaving the layer spacing and tilt angle un-

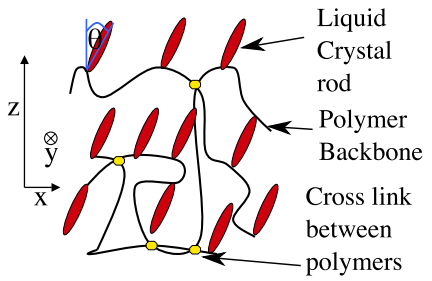

FIG. 1. (Color online) A Sm-C elastomer. liquid crystal (LC).

changed. A soft stripe domain involves an unbroken interface between regions suffering two distinct soft deformations corresponding to two different degrees of director rotation. We show that it is possible to form stripe domains with regions which have undergone any two degrees of director rotation relative to the polymer network. In fact, we show that given any pair of director rotations, it is possible to form two different stripe domains which form the two categories with distinct mechanical, geometric, and electrical properties described below. All stripes domains in Sm-C elastomers belong to one of these categories.

The first category of stripe domains is shown in Fig. 2. It has the property that the smectic layer plane transforms to the same plane under both deformations so the smectic layers are unbent at the texture boundaries. However, the two deformations are different, and this is indicated by the kinking of the initially straight sides of the sample. The director retains the same component parallel to the smectic layer normal (as it must for any soft deformation), but the components

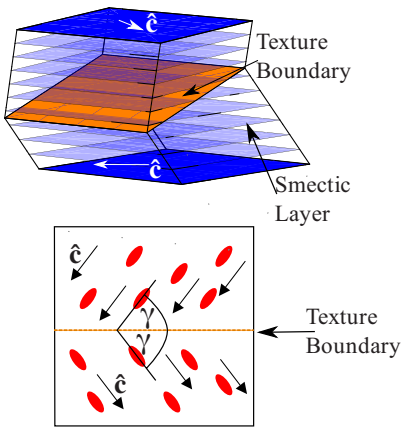

FIG. 2. (Color online) Top: a small region of a Sm-C elastomer after the formation of the first category of stripe domain. The region was cuboidal before deformation and has undergone different soft deformations on either side of the orange boundary plane. The smectic layers, which deform affinely, pass through the boundary without being bent. This figure was drawn with the material parameters $r=25$ and $\theta=0.6$. Bottom: a top view of a square region of a smectic layer that passes through the boundary, which is shown as an (orange) dashed line. The ovals represent the projection of the liquid-crystal rods in the plane and the arrows show the projection of the liquid-crystal director in the plane. The component of the LC director in the smectic plane, which we call $\hat{\mathbf{c}}$, is also shown in white on the top figure.

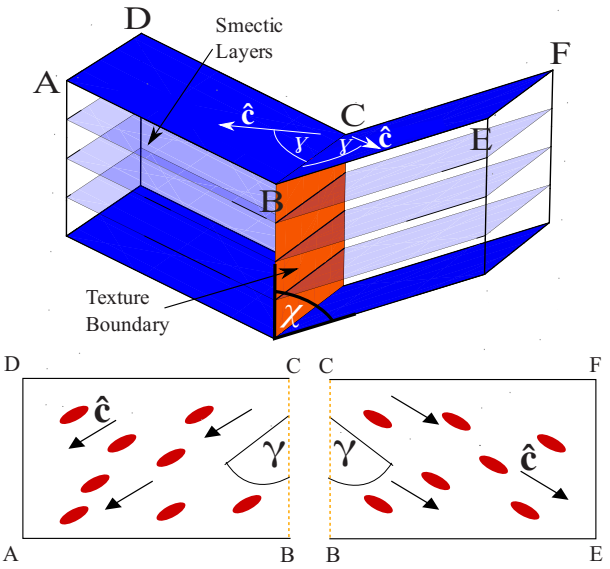

FIG. 3. (Color online) Top: a small region of a sample of Sm-C elastomer after the formation of the second type of stripe domain. Before deformation the sample was cuboidal. In this type of stripe domain, the smectic layers are bent at the boundary. This figure was drawn with the material parameters $r=25$ and $\theta=0.6$. Bottom: the two halves of the region on top each viewed down its smectic layer normal. The red ovals are the components of the LC rods in the LC layer plane and the black arrows are the components of the LC director in the LC layer plane. The component of the LC director in the smectic plane, which we call $\hat{\mathbf{c}}$, is also shown in white on the top figure.

in the layer form equal angles γ with the texture interfaces measured through the smectic layer plane—γ is the angle between the component of the smectic director in the smectic plane and the line of intersection between the interfacial and smectic planes. If the angle between the boundary and smectic layer planes is χ and the angle between the director and the layer normal is θ (which is a constant for all soft modes depending on the elastomers temperature and composition) then, for this first category of stripe domain,

$$\tan(\chi) = \tan(\theta)\sin(\gamma). \tag{2.1}$$

Textures of this type were predicted in [5].

The second category of stripe domain is shown in Fig. 3. In this category, the smectic layers are bent at the texture boundary as shown. Defining χ again as the angle between the smectic layers and the interface, the layers are bent by $\pi-2\chi$ at the interfaces. Defining γ as the angle between the component of the director in the smectic plane and the texture interface measured through the smectic plane, again the director forms equal angles on either side of the interface. For this category of stripe domains, the relationship between χ and γ is

$$\sin(\gamma) = \frac{(r-1)\cos^2(\theta)+1}{(1-r)\sin(\theta)\cos(\theta)}\cot(\chi) \tag{2.2}$$

where r is the anisotropy ratio of the step length tensor, and θ are constants for a given composition and temperature.

After the formation of a stripe-domain, there is a relative shear across the boundary indicated by the kinking of lines which were straight before deformation. We also characterize this relative shear by calculating the size of the kink in an initially straight line that after the formation of a stripe domain is normal to the boundary on one side of the boundary. This is a good characterization of the relative shear because it is the line that forms the largest kink at the boundary [7].

In the case of a Sm-C^* (chiral) elastomer which is polarized along the cross product of the layer normal and the director, the discontinuities across the texture boundary may give rise to a polarization. We show that the texture boundary is charged in a category one stripe domain (shown in Fig. 2) but not in a category two stripe domain (shown in Fig. 3). This is evident by examining the bottom of Figs. 2 and 3 and recalling that the interface will be charged if there is a discontinuity in the component of the polarization perpendicular to the boundary.

III. SOFT MODES

A. Choice of a reference state

The description of a deformation requires a reference state from which to measure deformations. For the purposes of this paper, it is useful to consider two states and two sets of axes. The first is a physically meaningful relaxed Sm-C^* elastomer, with the z axis along the layer normal, the x axis along the projection of the director into the layers, and the y axis into the page such that the three form a right-handed orthogonal set (see Fig. 1). The liquid-crystal director in this state will be $\mathbf{n}_0$. The neoclassical theory of Warner and Adams [3] predicts that if a deformation gradient $\boldsymbol{\lambda}$ is applied to this relaxed state, producing a state with director $\mathbf{n}$, providing the layer spacing and tilt angle are preserved, the free energy of the elastomer will be

$$F = \min_{\hat{\mathbf{n}}} \frac{\mu}{2} Tr(\boldsymbol{l}_0 \boldsymbol{\lambda}^T \boldsymbol{l}_1^{-1} \boldsymbol{\lambda}), \tag{3.1}$$

where $\boldsymbol{l}=(r-1)\boldsymbol{n}\otimes\boldsymbol{n}+\boldsymbol{I}$ and both r (the polymer anisotropy) and μ (an elastic modulus) are scalar constants of the material.

This relaxed state has extremely low symmetry. It is useful to use a higher-symmetry state as the reference state. To this end, we consider the fictitious state formed by applying the deformation $\boldsymbol{l}_0^{-1/2}$ to the relaxed state. In this fictitious state, the polymers have an isotropic conformation distribution, which gives this state higher symmetry. However, it is still layered; the new layer normal $\mathbf{b}$ is given by

$$\mathbf{b} = \frac{\boldsymbol{l}_0^{1/2}\mathbf{z}}{|\boldsymbol{l}_0^{1/2}\mathbf{z}|} = \mathbf{z}'. \tag{3.2}$$

We define a new primed set of axes in this state; the z' axis lies along the new layer normal, the y' axis coincides with the y axis, and the x' axis is chosen to make the set a right-handed orthogonal set. It lies in the new layer to y (see Fig. 4). This state will be used as the reference state and deformations from it will be written as $\boldsymbol{\Lambda}$. The free energy associated with a deformation $\boldsymbol{\Lambda}$ from this new state can be found

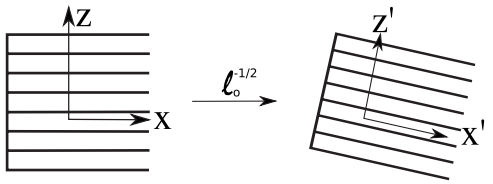

FIG. 4. Primed axes defined after deformation.

by substituting $\boldsymbol{\lambda}=\boldsymbol{\Lambda}\boldsymbol{l}_0^{-1/2}$ into Eq. (3.1) to give

$$F = \min_{\hat{\mathbf{n}}} \frac{\mu}{2} \mathrm{Tr}(\boldsymbol{\Lambda}^T \boldsymbol{l}^{-1} \boldsymbol{\Lambda}). \tag{3.3}$$

This expression is independent of $\mathbf{n}_0$. This makes identification and characterization of the soft modes easy.

B. Soft modes

For nematic (unlayered) elastomers, a deformation takes the reference state to a relaxed state if and only if it can be written in the form $\mathbf{Q_1}\boldsymbol{l}_0^{1/2}\mathbf{Q_2}$ [8], where $\mathbf{Q_1}$ and $\mathbf{Q_2}$ are rotations. This result has a simple interpretation. The deformation $\boldsymbol{l}_0^{1/2}$ returns the original relaxed state. However, for the unlayered case, the reference state is, for the purposes of elasticity, effectively isotropic—there is no $\mathbf{n}_0$ dependence in the energy [Eq. (3.3)] or any other coupling between reference state directions and the deformation gradient. This does not mean the state itself is physically isotropic—the liquid-crystal order is still present—but the isotropy of the polymer conformation distribution means that the energy of the elastomer does not depend on the direction of its alignment. This means that first rotating the reference state then applying $\boldsymbol{l}_0^{1/2}$ must also return a relaxed state. Finally, rotating the sample after applying $\boldsymbol{l}_0^{1/2}$ is just a body rotation and does not change the elastomers energy. Therefore, any deformation of the form $\mathbf{Q_1}\boldsymbol{l}_0^{1/2}\mathbf{Q_2}$ must return a relaxed elastomer.

To find the soft deformations for a Sm-C elastomer, we must simply find the subset of these deformations that obey the constraint that the relaxed layer spacing and director tilt angle are preserved. Therefore, similarly to the nematic case, any deformation of the form

$$\mathbf{Q_1}\boldsymbol{l}_0^{1/2}\mathbf{B}, \tag{3.4}$$

where $\boldsymbol{B}$ is a rotation of any angle about $\mathbf{b}$ must return a relaxed elastomer. This is in fact the complete set of soft deformations since these are the only deformations that are consistent with preserving the layer spacing.

If $\boldsymbol{\Lambda}_s$ is to return the original layer spacing (which is the same as returning the original layer area since volume is conserved), it must satisfy

$$|\boldsymbol{\Lambda}_s^{-T}\mathbf{b}| = |\boldsymbol{l}_0^{-1/2}\mathbf{b}|,$$

where $-T$ denotes the inverse transpose, which is how plane normals (or vector areas) transform.

Substituting a generic unlayered soft mode for $\boldsymbol{\Lambda}_s$ gives

$$|\mathbf{Q}_1\boldsymbol{l}_0^{-1/2}\mathbf{Q}_2\mathbf{b}| = |\boldsymbol{l}_0^{-1/2}\mathbf{b}|. \tag{3.5}$$

The rotation $\mathbf{Q}_1$ does not change the modulus of the vector $\boldsymbol{l}_0^{-1/2}\mathbf{Q}_2\mathbf{b}$ so this condition can be written as

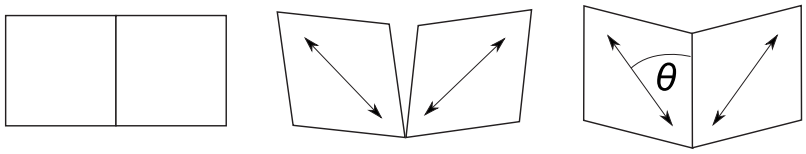

FIG. 5. Left: a block of nematic elastomer in the reference configuration split into two regions. Middle: uniaxial stretches are applied in the two regions. The boundary is stretched to the same degree by both stretches provided the boundary line bisects the two axes; however, the material still rips at the boundary. Right: a body rotation of the two regions can restore material continuity because the boundary was stretched by the same amount under both deformations. The strains in the third direction (out of the page) also match because this direction is perpendicular to both axes, so the interfacial plane normal is in the same plane as the two axes and bisects them.

$$|\boldsymbol{l}_0^{-1/2}\mathbf{Q}_2\mathbf{b}| = |\boldsymbol{l}_0^{-1/2}\mathbf{b}|.$$

As $\boldsymbol{l}_0$ and all its powers are uniaxial matrices with their axes aligned with the liquid-crystal director $\mathbf{n}_0$, this equality will hold only for $\mathbf{Q}_2$ that map $\mathbf{b}$ to one of the two cones formed by rotating $\mathbf{b}$ and $-\mathbf{b}$ around $\mathbf{n}_0$. The set of such rotations is completely parametrized by

$$\mathbf{Q}_2 = \mathbf{N}\mathbf{R}_\mathbf{y}\mathbf{B},$$

where the rotations $\mathbf{N}$ and $\mathbf{B}$ can be by any angle (about $\mathbf{n}_0$ and $\mathbf{b}$, respectively), and, just in this section, $\mathbf{R}_\mathbf{y}$ can be either a rotation of π about $\mathbf{y}$ or the identity operator. Intuitively, $\mathbf{B}$ does not change $\mathbf{b}$, $\mathbf{R}_\mathbf{y}$ determines which cone $\mathbf{b}$ is mapped to, and $\mathbf{N}$ determines where on the cone $\mathbf{b}$ is mapped to. Since both $\mathbf{N}$ and $\mathbf{R}_y$ commute with $\boldsymbol{l}_0$ and therefore can be incorporated into $\boldsymbol{Q}_1$, we see that any soft deformation must be of form (3.4). Since all deformations of this form are soft, this is the complete set.

Nematic liquid-crystal phases are defined by a singe axis—the nematic director—so in this case the $\boldsymbol{l}_0$ tensor must be uniaxial with its axis along the director as assumed above. However, Sm-*C* phases are defined by two axes—the smectic director and the layer normal—so the $\boldsymbol{l}_0$ tensor will in reality be to some extent biaxial. Here we follow Adams and Warner [3,5] and neglect this biaxiality since the uniaxial approximation already predicts very rich soft behavior. However, in Appendix C, we show that the addition of biaxiality to the system will not significantly change the results since the existence, uniqueness, and charge properties of the two types of stripe domain are unaffected.

IV. GEOMETRIC PERSPECTIVE

In the following sections, the existence, uniqueness, and properties of the two families of stripe domain described in the results section will be proved algebraically. The algebraic approach is very powerful because it uses theorems developed in the study of martensitic metals to establish the uniqueness of the set of solutions described, allowing us to be confident that there are no other stripe domains with different morphologies. However, it is possible to think about the problem completely geometrically. First we consider a simple unlayered (nematic) system in the reference configuration. The energy of the sample is minimized by a uniaxial stretch by $r^{1/3}$ along any axis. The nematic director aligns with the axis of the stretch. If we apply two different minimizing stretches in different parts of the sample then if the material is to not rip, there must be a plane between the two regions that undergoes the same deformation under both stretches. The direction perpendicular to both axes is stretched by the same amount ($r^{-1/6}$) by both stretches so this is one of the directions in the interfacial plane. To find the other, we consider the plane containing both axes. Provided in this plane the boundary between the two regions bisects the two axes then it is stretched to the same degree by both deformations. The two stretches still cause the boundary to rip, but because it has been stretched to the same degree by both stretches, the two parts can be body rotated back together to restore the continuity of the body. This is shown in Fig. 5. This construction leads to a simple conclusion—a stripe domain can form provided the interfacial plane normal bisects the two liquid-crystal directors.

In the Sm-*C* case, the reference configuration is layered, and the minimizing stretches must make a fixed angle with the layer normal. However, the conclusion in the nematic case is still valid—the interfacial plane normal must bisect the two directors. Figure 6 shows the analogous construction for Sm-*C* elastomers. The plane of the diagram, which is the plane containing the two smectic directors, in general, makes an angle with the smectic planes shown as dotted lines. The requirement that the smectic director makes a fixed angle with the smectic planes means that, in the plane drawn, both smectic directors must make equal angles with the dotted lines. There are therefore only two directions that bisect the smectic directors which give rise to the two categories of stripe domain: one which causes the layers to kink at the boundary and one that does not (see Fig. 6). We could now use these constructions to recover the complete morphology. For example, in the last diagram of Fig. 6, if we set up an orthogonal basis in which the layer normal is (0,0,1) and the line of intersection between the layer plane and the interfacial plane is (0,1,0) then the two smectic directors are $(\pm\sin\theta\sin\gamma, \sin\theta\cos\gamma, \cos\theta)$. The interfacial normal bisects these directors giving $(0, \sin\theta\cos\gamma, \cos\theta)$; so, if χ is the angle between the interfacial plane and the smectic layers, we can immediately recover our first main result [Eq. (2.1)]. It would be possible to peruse this construction and predict the complete morphology of the two types of twin; but here we complete the description using the more powerful algebraic approach.

V. CONTINUITY ACROSS THE STRIPE-DOMAIN BOUNDARY

If a sample in the reference state is split into two regions separated by a plane with normal $\mathbf{m}$ and one region is sub-

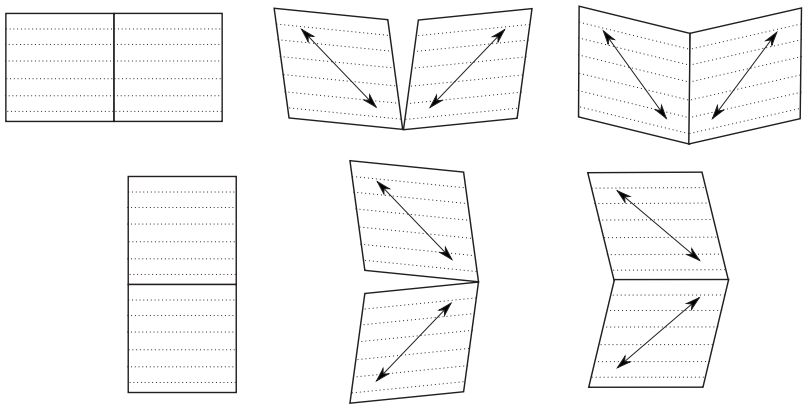

FIG. 6. The same construction as Fig. 5 but for smectic elastomers. Top left: a slice through a block of Sm-*C* elastomer in the reference state. The smectic planes are shown as dotted lines. The slice is at an angle to the planes so the planes are not, in general, either perpendicular or parallel to the slice. Middle: two uniaxial stretches are applied in the two regions. As in the nematic case the boundary must bisect the axes, but in this case the axes must also make equal angles with the dotted lines to ensure the smectic director makes the preferred tilt angle with the layer normal. As before this rips the material. Top right: since the boundary is stretched to the same degree by both stretches material continuity can be restored by body rotations. The resulting structure has the layers bent at the boundary. Bottom: the same construction again but with the other possible bisecting boundary. In this case the layers are not bent at the boundary.

jected to a deformation $\mathbf{\Lambda}_1$ and the other to $\mathbf{\Lambda}_2$, the condition that the sample remains continuous (rank one connected) is that there is a vector $\mathbf{a}$ such that

$$\mathbf{\Lambda}_1 - \mathbf{\Lambda}_2 = \mathbf{a} \otimes \mathbf{m}. \tag{5.1}$$

Physically, $\mathbf{a}$ is a vector in the plane of the boundary after deformation. This is illustrated in Fig. 7. A detailed explanation of texture and the continuity equation can be found in [7]. This structure is known as a twin. A full stripe domain is simply many repetitions of the same twin so that the deformation alternates in stripes separated by parallel plane boundaries.

The principal result in this section is that given any two of the soft modes of deformation $\mathbf{\Lambda}_{1,s}$ and $\mathbf{\Lambda}_{2,s}$, there are two rotations $\mathbf{Q}$ and $\mathbf{Q}'$, such that the deformations $\mathbf{\Lambda_1}=\mathbf{Q}\mathbf{\Lambda}_{1,s}$ and $\mathbf{\Lambda_1}=\mathbf{Q}'\mathbf{\Lambda}_{1,s}$ can both satisfy Eq. (5.1) with $\mathbf{\Lambda_2}=\mathbf{\Lambda}_{2,s}$, and hence can both form a stripe domain with $\mathbf{\Lambda}_{2,s}$. For Eq. (5.1) to hold, $\mathbf{Q}$ and $\mathbf{Q}'$ require different $\mathbf{a}$ and $\mathbf{m}$. The required $\mathbf{m}$ is also calculated explicitly. To do this, we use two theorems (discussed in [7]) to the continuity equation. The first, a uniqueness theorem proved by James and Ball [9] states that if $\mathbf{Q}$ is a rotation, $\mathbf{\Delta}$ and $\mathbf{\Gamma}$ are distinct deformations, and $\mathbf{m}$ and $\mathbf{a}$ are vectors, the equation

$$\mathbf{Q\Delta} - \mathbf{\Gamma} = \mathbf{a} \otimes \mathbf{m}, \tag{5.2}$$

for fixed $\mathbf{\Delta}$ and $\mathbf{\Gamma}$ has either zero or two solutions. The two solutions will in general have different $\mathbf{Q}$, $\mathbf{m}$, and $\mathbf{a}$.

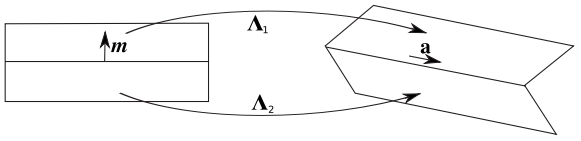

FIG. 7. A different deformation is applied on each side of a plane boundary. A stripe domain is simply many repetitions of this structure so that the deformation alternates in stripes separated by parallel plane boundaries.

The second theorem is known as Mallard's law and states that [10,7] if, for a *pair of distinct deformations* $\mathbf{\Delta}$ and $\mathbf{\Gamma}$ there exists a rotation $\mathbf{Q}_3$ and a π rotation $\mathbf{R}$ such that

$$\mathbf{\Delta} = \mathbf{Q}_3\mathbf{\Gamma R}, \tag{5.3}$$

then there are certainly two (not zero) solutions to Eq. (5.2). These *solutions* can be computed relatively easily—if the *axis* of $\mathbf{R}$ is $\mathbf{s}$ then the two solutions are

$$\text{I.} \quad \mathbf{a} = 2\left(\frac{\mathbf{\Gamma}^{-T}\mathbf{s}}{|\mathbf{\Gamma}^{-T}\mathbf{s}|^2} - \mathbf{\Gamma s}\right), \quad \mathbf{m} = \mathbf{s}, \tag{5.4}$$

$$\text{II.} \quad \mathbf{a} = \tilde{\rho}\mathbf{\Gamma s}, \quad \mathbf{m} = \frac{2}{\tilde{\rho}}\left(\mathbf{s} - \frac{\mathbf{\Gamma}^T\mathbf{\Gamma s}}{|\mathbf{\Gamma s}|^2}\right), \tag{5.5}$$

where $\tilde{\rho}$ is chosen to make $\mathbf{m}$ a unit vector.

Substituting soft-mode expressions for $\mathbf{\Lambda}_1$ and $\mathbf{\Lambda}_2$ from Eq. (3.4) gives

$$\mathbf{Q}_1 l_0^{1/2}\mathbf{B}_{b_1} - \mathbf{Q}_2 l_0^{1/2}\mathbf{B}_{b_2} = \mathbf{a} \otimes \mathbf{m} \tag{5.6}$$

(here $\mathbf{Q}_1$ and $\mathbf{Q}_2$ are arbitrary rotations). More specialized forms for $\mathbf{\Lambda}_1$ and $\mathbf{\Lambda}_2$ can be adopted since none of the intrinsic properties of a texture are changed by rotating the whole sample about any axis after deformation or around $\mathbf{b}$ (the reference state layer normal) in the reference state. Only the relative rotation between the two regions at each stage $\mathbf{Q_1Q_2^T}$ and $\mathbf{B}_{b_1}\mathbf{B}_{b_2}^T$ are physically important. Therefore, we can limit our attention from all equations of form (5.6) to any subset that still includes all possible relative rotations $\mathbf{Q_1Q_2^T}$ and $\mathbf{B}_{b_1}\mathbf{B}_{b_2}^T$. One such subset is given by

$$\mathbf{Q}l_0^{1/2}\mathbf{B}_b - l_0^{1/2}\mathbf{B}_{-b} = \mathbf{a} \otimes \mathbf{m}. \tag{5.7}$$

This form (with $\mathbf{Q_2}=\mathbf{I}$) is useful because Mallard's law can be directly applied to it. The choice to split the relative rotation about $\mathbf{b}$ in the reference state (the $\mathbf{B}$ rotations) equally between the two regions is motivated by algebraic convenience.

Equation (5.7) will only be satisfied by very special combinations of $\mathbf{Q}$, b, $\mathbf{a}$, and $\mathbf{m}$. To find these combinations (solve the continuity equation), we use Mallards law. Comparing Eqs. (5.2) and (5.3) with Eq. (5.7), we see that there will be Mallard's law type solutions to Eq. (5.7) if we can find any rotation $\mathbf{Q}_3$ and any π rotation $\mathbf{R}$ such that

$$\boldsymbol{l}_0^{1/2}\mathbf{B}_b = \mathbf{Q}_3\boldsymbol{l}_0^{1/2}\mathbf{B}_{-b}\mathbf{R}. \tag{5.8}$$

This holds if $\mathbf{Q}_3=\mathbf{R}=\mathbf{R}_\mathbf{y}$ because $\mathbf{y}$ is perpendicular to $\mathbf{b}$ and $\mathbf{n}_0$ and so $\mathbf{B}_{-b}\mathbf{R}_\mathbf{y}=\mathbf{R}_\mathbf{y}\mathbf{B}_b$ and $\mathbf{R}_\mathbf{y}\boldsymbol{l}_0^{1/2}\mathbf{R}_\mathbf{y}=\boldsymbol{l}_0^{1/2}$.

This result is significant. As continuity (5.7) is of form (5.2), it can, by the uniqueness theorem, have either two or zero solutions for each value of b (varying $\mathbf{Q}$, $\mathbf{a}$, and $\mathbf{m}$). Mallard's law is satisfied for all b [since with the right choice of $\mathbf{Q_3}$ and $\mathbf{R}$, Eq. (5.8) is satisfied for all b] so the continuity equation has two (rather than zero) solutions for all b. This is the largest possible set of solutions. This means that any two soft deformations can, if rotated correctly relative to each other, form two different stripe domains, giving rise to the two classes of stripe domains described in this paper.

At this stage, we could simply calculate the mechanical properties of both the solutions for each value of b using Eqs. (5.4) and (5.5). However, calculating the first of these solutions is significantly simpler than calculating the second since its boundary normal is simply the axis of $\boldsymbol{R}$. We can avoid calculating the mechanical properties of the solution in this way by finding another $\mathbf{Q_3}$ and $\mathbf{R}$ that satisfy Eq. (5.8). This can be done by noticing that Eq. (5.3) can be rewritten as

$$\boldsymbol{\Delta}^T\boldsymbol{\Delta} = \mathbf{R}\boldsymbol{\Gamma}^T\boldsymbol{\Gamma}\mathbf{R}.$$

Casting Eq. (5.8) in this form and moving all rotations to the right-hand side gives

$$\boldsymbol{l}_0 = \mathbf{B}_b\mathbf{R}\mathbf{B}_b\boldsymbol{l}_0\mathbf{B}_{-b}\mathbf{R}\mathbf{B}_{-b}.$$

The expression on the right-hand side is a rotated form of $\boldsymbol{l}_0$; the rotation will not change $\boldsymbol{l}_0$, (and hence the equality will hold) if the rotation does not change the axis of $\boldsymbol{l}_0$, giving

$$\mathbf{n}_0 = \pm\,\mathbf{B}_b\mathbf{R}\mathbf{B}_b\mathbf{n}_0. \tag{5.9}$$

For fixed $\mathbf{n}_0$ and $\mathbf{b}$, this has two solutions for $\mathbf{R}$, one for each sign. The minus sign is given by the $\mathbf{R}=\mathbf{R}_\mathbf{y}$ solution found above. This follows as

$$\mathbf{B}_b\mathbf{R}_\mathbf{y}\mathbf{B}_b = \mathbf{B}_b\mathbf{B}_{-b}\mathbf{R}_\mathbf{y} = \mathbf{R}_\mathbf{y},$$

and

$$\mathbf{R}_\mathbf{y}\mathbf{n}_0 = -\,\mathbf{n}_0.$$

The solution for the plus sign is rather more complex as it depends on b. As $\mathbf{n}_0$ lies in the x'-z' plane (which is the same as the x-z plane), it can be decomposed into components along $\mathbf{x}'$ and $\mathbf{b}$. Writing

$$\mathbf{n}_0 = e\mathbf{x}' + d\mathbf{b},$$

we see that

$$\mathbf{B}_b\mathbf{n}_0 = e[\cos(b)\mathbf{x}' + \sin(b)\mathbf{y}] + d\mathbf{b}$$

and

$$\mathbf{B}_{-b}\mathbf{n}_0 = e[\cos(b)\mathbf{x}' - \sin(b)\mathbf{y}] + d\mathbf{b}.$$

Since Eq. (5.9) rearranges (with the plus sign) to give

$$\mathbf{B}_{-b}\mathbf{n}_0 = \mathbf{R}\mathbf{B}_b\mathbf{n}_0,$$

$\mathbf{R}$ must map these two vectors onto each other. As it is a rotation of π, this uniquely identifies the axis or rotation as the average of unit vectors in these two directions. Defining the axis as the unit vector $\mathbf{s}$, it can be written as

$$\mathbf{s} \propto d\mathbf{b} + e\,\cos(b)\mathbf{x}'.$$

For a given b, there are two $\mathbf{R}$ that satisfy Mallard's law. Each $\mathbf{R}$ generates two solutions to continuity (5.7), suggesting there might be four solutions in total. However, there can only be two solutions so the two solutions generated by each $\mathbf{R}$ must be the same. The first solution for each $\mathbf{R}$ is very easy to calculate as the reference state boundary normal $\mathbf{m}$ is along the rotation axis of $\mathbf{R}$. This suggests we only need to calculate this easy first solution for each $\mathbf{R}$; provided these two solutions are different, we will then have two solutions to the continuity equation. As we know there are precisely two solutions, this is all the solutions. If we were to calculate the second solution for one $\mathbf{R}$, we would find it coincided with the first solution from the other.

VI. CHARACTERIZATION OF THE STRIPE DOMAINS

In the previous section, it was shown that all physically distinct stripe domains can be formed between two soft modes of deformation of the form $\boldsymbol{\Lambda}_\mathbf{1}=\mathbf{Q}\boldsymbol{l}_0^{1/2}\mathbf{B}_b$ and $\boldsymbol{\Lambda}_\mathbf{2}=\boldsymbol{l}_0^{1/2}\mathbf{B}_{-b}$. Further, using Mallard's law, it was shown that for each value of b there are two rotations $\mathbf{Q}$ ($\mathbf{Q_1}$ and $\mathbf{Q_2}$) such that $\boldsymbol{\Lambda}_\mathbf{1}$ and $\boldsymbol{\Lambda}_\mathbf{2}$ can form a stripe domain. If the texture is to form properly, the correct boundary normal in the reference configuration ($\mathbf{m}$ in Fig. 7) must be used. These are $\mathbf{m}_1 \propto d\mathbf{b}+e\,\cos(b)\mathbf{x}'$ (when $\mathbf{Q}=\mathbf{Q_1}$) and $\mathbf{m}_2=\mathbf{y}$ (when $\mathbf{Q}=\mathbf{Q_2}$).

Before the physical properties of the stripe domains can be calculated, the rotations $\mathbf{Q_1}$ and $\mathbf{Q_2}$ must be determined so that the deformations giving rise to the textures are completely specified. This can be done using the continuity equation and the requirement that $\mathbf{m}$ must transform to the same vector under both deformations in a stripe domain (because the transformed $\mathbf{m}$ is the boundary normal in the final state).

Once the deformations are fully determined, the liquid-crystal director, the liquid-crystal layer normal, and the texture boundary normal in the final state can be calculated on both sides of the interface to reveal its physical structure. Since in general the surface normal $\mathbf{k}$ transforms under the deformation $\boldsymbol{\Gamma}$ to $\boldsymbol{\Gamma}^{-T}\mathbf{k}$ ($-T$ denotes the inverse transpose), the smectic layers on either side of the interface can be calculated by applying this rule to the layer normal in the reference state ($\mathbf{b}$) on either side of the interface. Similarly, the boundary normal in the final state can be calculated by applying this rule to $\mathbf{m}$, using either deformation in the stripe domain. Finding the position of the liquid-crystal director is a little more subtle; it is not defined in the reference state (in which the polymers have an isotropic conformation distribution) but is introduced when the $\boldsymbol{l}_0^{1/2}$ deformation is applied. As $\boldsymbol{l}_0^{1/2}$ is an extension along $\mathbf{n}_0$, it extends the polymer con-

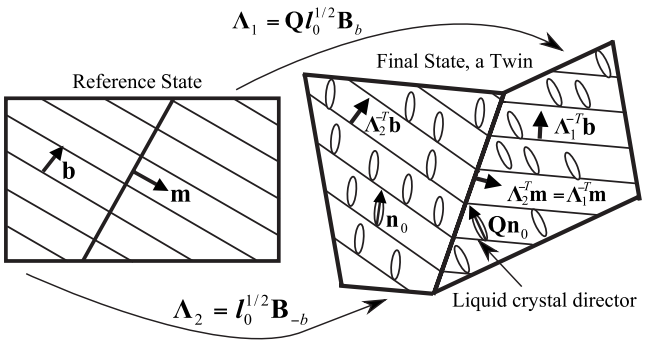

FIG. 8. A sample in the (layered) reference state is divided into two regions and different (but compatible) soft deformations are applied in each region. The deformations move the boundary between the regions and the layers and introduce an LC director in both regions.

formation distribution along $\mathbf{n}_0$ and introduces the director, also along $\mathbf{n}_0$. The director transforms as a line element under the subsequent rotations that complete the deformations. The full set of properties is summarized in Fig. 8. Although the calculations indicated above are straightforward, they are also rather long, not least because to describe fully each class of stripe domain five quantities must be calculated, giving ten calculations in all. The full set of calculations is given in Appendix A. The resulting mechanical structure of the stripe domains was given in Sec. II.

There is one other more subtle mechanical feature of the stripe domains that is worth characterizing: the amount of shear across the boundary. The continuity equation [Eq. (5.1)] can be written as

$$\mathbf{\Lambda}_1 = (\mathbf{I} + \mathbf{a} \otimes \mathbf{\Lambda}_2^{-T}\mathbf{m})\mathbf{\Lambda}_2, \tag{6.1}$$

where the matrix premultiplying $\mathbf{\Lambda}_2$ is a simple shear. This means that to change a region which has suffered a deformation $\mathbf{\Lambda}_2$ to one which has suffered a deformation $\mathbf{\Lambda}_1$, one need only to apply a simple shear, and this is what we mean by the shear across the interface. It is associated with the shear angle ζ, where

$$\tan(\zeta) = |\mathbf{a}||\mathbf{\Lambda}_1^{-T}\mathbf{m}| = |\mathbf{a}||\mathbf{\Lambda}_2^{-T}\mathbf{m}|. \tag{6.2}$$

If a straight line is embedded in the sample in the reference state, it will kink at the boundary after deformation. Physically, the shear angle is the amount such a line kinks if after deformation it is normal to the boundary on one side of the boundary [7].

For Mallard's law type stripe domains, this is the same for both type-1 and type-2 solutions and evaluates to

$$\tan(\zeta) = 2\sqrt{|\mathbf{\Lambda}_2\mathbf{m}|^2|\mathbf{\Lambda}_2^{-T}\mathbf{m}|^2 - 1}, \tag{6.3}$$

which can easily be verified by substituting the solutions for each type of solution [Eqs. (5.4) and (5.5)] into Eq. (6.2). This means that ζ will be the same for both stripe domains (one in each class) generated using a given value of b. A plot of $\tan(\zeta)$ against b is shown in Fig. 9 and details of the calculation of the curve can be found at the end of Appendix A.

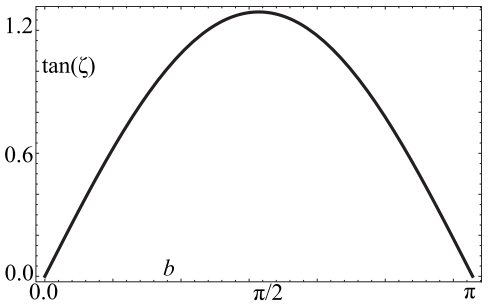

FIG. 9. Shear angle across the boundary for both classes of stripe domain as a function of b plotted with $r=25$ and $\theta=0.6$; the maximum shear angle is $\tan(\zeta)=(r-1)\sin(2\theta)/[(r-1)\cos^2(\theta)+1]$ and occurs at $b=\pi/2$.

VII. FERROELECTRIC PROPERTIES OF THE STRIPE DOMAINS

At the texture boundaries, there is a discontinuity in the liquid-crystal director, and hence, for Sm-C^* elastomers, a discontinuity in the electrical polarization (which is along the cross product of the layer normal and the director); so it is possible that the texture boundaries are charged.

The main result of this section is that the class two stripe domains (generated by the **y** axis of rotation) are uncharged, and the class one stripe domains [generated by the $d\mathbf{b} + e\cos(b)\mathbf{x}'$ axis] are charged. Since both the directors and layer normals in each stripe domain have already been calculated, this could be proved very simply by taking the pertinent cross products; but here we prove and use a more general result.

Consider two deformations $\mathbf{Q}_1\mathbf{\Lambda}_1$ and $\mathbf{\Lambda}_2$ that act on two regions separated by a plane boundary with normal $\mathbf{m}$ in the reference configuration. Let the boundary normal be $\mathbf{m}'$ in the final state. The continuity condition gives

$$\mathbf{Q}_1\mathbf{\Lambda}_1 - \mathbf{\Lambda}_2 = \mathbf{a}' \otimes \mathbf{m}.$$

If the deformation $\mathbf{\Lambda}_1$ results in a polarization $\mathbf{p}_1$ and the deformation $\mathbf{\Lambda}_2$ results in a polarization $\mathbf{p}_2$ (which subsequently transform as line elements) then the condition that the texture boundary is not charged is that the component of the polarization normal to the boundary is continuous across the boundary,

$$(\mathbf{Q}_1\mathbf{p}_1 - \mathbf{p}_2) \cdot \mathbf{m}' = 0.$$

If the stripe domain obeys Mallard's law then

$$\mathbf{\Lambda}_1 = \mathbf{Q}_2\mathbf{\Lambda}_2\mathbf{R}, \tag{7.1}$$

and if

$$\mathbf{p}_1 = \mathbf{Q}_2\mathbf{p}_2, \tag{7.2}$$

the first Mallard's law solution will not be charged and the second will be. The proof is simple. First, we make the following rearrangement:

$$\mathbf{p}_1 = \mathbf{Q}_2\mathbf{p}_2,$$

$$\mathbf{\Lambda}_1^{-1}\mathbf{p}_1 = (\mathbf{Q}_2\mathbf{\Lambda}_2\mathbf{R})^{-1}\mathbf{Q}_2\mathbf{p}_2,$$

$$\mathbf{\Lambda}_1^{-1}\mathbf{p}_1 = \mathbf{R}\mathbf{\Lambda}_2^{-1}\mathbf{p}_2,$$

$$(\mathbf{\Lambda}_1^{-1}\mathbf{p}_1)\cdot\mathbf{m} = (\mathbf{R}\mathbf{\Lambda}_2^{-1}\mathbf{p}_2)\cdot\mathbf{m}.$$

Second, we use the fact that we know $\mathbf{m}$ for a general Mallard's law stripe domain—for the first Mallard's law solution $\mathbf{m}$ is along the axis of $\mathbf{R}$ so $(\mathbf{R}\mathbf{\Lambda}_2^{-1}\mathbf{p}_2)\cdot\mathbf{m}=(\mathbf{\Lambda}_2^{-1}\mathbf{p}_2)\cdot\mathbf{m}$. For the second solution, $\mathbf{m}$ is perpendicular to the axis of $\mathbf{R}$ so $(\mathbf{R}\mathbf{\Lambda}_2^{-1}\mathbf{p}_2)\cdot\mathbf{m}=-(\mathbf{\Lambda}_2^{-1}\mathbf{p}_2)\cdot\mathbf{m}$. These results can be written as

$$(\mathbf{\Lambda}_1^{-1}\mathbf{p}_1)\cdot\mathbf{m} = \pm(\mathbf{\Lambda}_2^{-1}\mathbf{p}_2)\cdot\mathbf{m},$$

which can be rewritten as

$$\mathbf{Q}_1\mathbf{p}_1\cdot(\mathbf{Q}_1\mathbf{\Lambda}_1)^{-T}\mathbf{m} = \pm\,\mathbf{p}_2\cdot\mathbf{\Lambda}_2^{-T}\mathbf{m}.$$

However, $\mathbf{m}$ transforms to $\mathbf{m}'$ under both $\mathbf{Q}_1\mathbf{\Lambda}_1$ and $\mathbf{\Lambda}_2$ so

$$(\mathbf{Q}_1\mathbf{p}_1 \mp \mathbf{p}_2)\cdot\mathbf{m}' = 0.$$

Therefore, the first Mallard's law solution is uncharged and the second is charged. This result suggests that a structure of two classes of stripe domains, one of which is charged and one of which is neutral, may be quite widespread in ferroelectric systems. We note that in occasional degenerate cases (if $\mathbf{Q}_1\mathbf{p}_1$ and $\mathbf{p}_2$ are parallel), the above condition is consistent with both classes being uncharged. The disproportionation stripe domain discussed in [5] is such an example.

Returning to Sm-C^* elastomers, if $\mathbf{\Lambda}_1$ and $\mathbf{\Lambda}_2$ are soft modes it was shown in Sec. V that there are two choices for $\mathbf{Q}_2$ and $\mathbf{R}$ that satisfy Eq. (7.1). The first choice [with the axis of $\mathbf{R}$ along $d\mathbf{b}+e\cos(b)\mathbf{x}'$ and, as shown in Appendix A, the axis of $\mathbf{Q_2}$ along $\mathbf{z}$] generates the class one stripe domains as its first solution and the class two stripe domains as its second solution. This order is reversed for the second choice (with the axis of $\mathbf{R}$ along $\mathbf{y}$ and $\mathbf{Q_2}=\mathbf{R}_y$).

Both $\mathbf{\Lambda}_1$ and $\mathbf{\Lambda}_2$ produce a state with a director along $\mathbf{n}_0$ and the layer normal along $\mathbf{z}$ so the polarization, which is given by the cross product of these two vectors, is along $\mathbf{y}$. The sign of the polarization is determined by the chirality of the rods. Setting $\mathbf{p}_1=\mathbf{p_2}=\mathbf{y}$, we see that Eq. (7.2) is satisfied by the second choice for $\mathbf{Q_2}$ and $\mathbf{R}$ but not the first. This means that the second class of stripe domains (which are the first solution for this choice of $\mathbf{Q}_2$ and $\mathbf{R}$) is not charged, while the first class of stripe domains (which are the second solution) are charged.

These results are easily demonstrated by explicitly calculating the polarizations for each category of stripe domain. Electrical actuation of these materials may be complicated by the formation of these laminate charge structures. This is discussed in more detail in [5].

VIII. CONCLUSIONS

A deformation of a Sm-C or Sm-C^* liquid-crystal elastomer is a soft mode if and only if it can be written in the form

$$\mathbf{\lambda} = \mathbf{Q}\boldsymbol{l}_0^{1/2}\mathbf{B}\boldsymbol{l}_0^{-1/2},$$

where $\boldsymbol{l}_0$ is the step length tensor in the initial (relaxed) state, $\mathbf{Q}$ is an arbitrary rotation, and, if $\mathbf{z}$ is the liquid-crystal layer normal, $\mathbf{B}$ is a rotation about $\boldsymbol{l}_0^{1/2}\mathbf{z}$.

Any two soft deformations can (if they are rotated appropriately relative to each other) form two stripe domains: both of which obey Mallard's law. This is the largest possible set of stripe domains. These two textures form two distinctive categories: one in which the LC layers are bent at the texture boundary and one in which the texture boundary is charged. If γ is the angle between the component of the LC director projected into the LC plane and the texture boundary (measured through the LC layer plane) and χ is the angle between the boundary normal and the LC layer normal then in the latter case

$$\tan(\chi) = \tan(\theta)\sin(\gamma),$$

and in the former case

$$\sin(\gamma) = \frac{(r-1)\cos^2(\theta)+1}{(1-r)\sin(\theta)\cos(\theta)}\cot(\chi).$$

In the two results above, θ (the angle between the director and the layer normal) and r (the anisotropy of the polymer conformation distribution) are constants for elastomers of a given chemical nature and temperature. Although the calculations were done using the unphysical reference state variable b, these results connect physical angles in the final state and hence have the potential to be tested experimentally.

ACKNOWLEDGMENTS

We are grateful for many interesting and important discussions with Professor Mark Warner. This work was carried out during various visits by J.S.B. to Caltech and K.B. to Cambridge. We gratefully acknowledge the financial support of the CamSURF program at Caltech, the Powell Foundation, the Sims Fund, and the EPSRC.

APPENDIX A: CALCULATION OF THE PHYSICAL PROPERTIES OF THE STRIPE DOMAINS

Before embarking on the calculations, it is useful to define a few additional variables

$$\rho = \cos^2(\theta)(r-1)+1, \tag{A1}$$

$$\alpha = (1-r)\sin(\theta)\cos(\theta), \tag{A2}$$

$$\beta = \cos^2(\theta)(r^2-1)+1, \tag{A3}$$

where r (the anisotropy of the polymer distribution) and θ (the angle between the LC director and layer normal) are constants of the material. A few results that will be used repeatedly are stated below,

$$\beta = \rho^2+\alpha^2 \quad d = \frac{\cos(\theta)\sqrt{r}}{\sqrt{\rho}} \quad e = \frac{\sin(\theta)}{\sqrt{\rho}},$$

$$\boldsymbol{l}_0^{-1/2}\mathbf{x}' = \sqrt{\frac{\rho}{r}}\mathbf{x}+\frac{\alpha}{\sqrt{\rho r}}\mathbf{z} \quad \boldsymbol{l}_0^{1/2}\mathbf{x}' = \sqrt{\frac{r}{\rho}}\mathbf{x},$$

$$\boldsymbol{l}_0^{-1/2}\mathbf{b} = \frac{1}{\sqrt{\rho}}\mathbf{z} \quad \boldsymbol{l}_0^{1/2}\mathbf{b} = \frac{-\alpha}{\sqrt{\rho}}\mathbf{x}+\sqrt{\rho}\mathbf{z},$$

$$\boldsymbol{l}_0^{-1/2}\mathbf{y} = \boldsymbol{l}_0^{1/2}\mathbf{y} = \mathbf{y} \quad \boldsymbol{l}_0^{1/2}\mathbf{z} = \sqrt{\rho}\mathbf{b},$$

$$\mathbf{x}' = \frac{1}{\sqrt{r\rho}}[\cos^2(\theta)(\sqrt{r}-1)+1]\mathbf{x} - \frac{(\sqrt{r}-1)}{\rho}\sin(\theta)\cos(\theta)\mathbf{z},$$

$$\mathbf{b} = \frac{1}{\sqrt{\rho}}\{(\sqrt{r}-1)\sin(\theta)\cos(\theta)\mathbf{x} + [\cos^2(\theta)(\sqrt{r}-1)+1]\mathbf{z}\}.$$

These results can easily be verified by expanding out the left-hand side in the x-y-z basis, for example, using the definition of $\mathbf{b}$ [Eq. (3.2)],

$$\boldsymbol{l}_0^{1/2}\mathbf{b} = \frac{\boldsymbol{l}_0\mathbf{z}}{|\boldsymbol{l}_0^{1/2}\mathbf{z}|}.$$

Remembering that $\mathbf{n_0}=[\sin(\theta),0,\cos(\theta)]$ (in the x-y-z basis) and $\boldsymbol{l}_0=(r-1)\boldsymbol{n}_0\otimes\boldsymbol{n}_0+\boldsymbol{I}$,

$$\boldsymbol{l}_0^{1/2}\mathbf{z} = (\sqrt{r}-1)(\mathbf{n_0}\cdot\mathbf{z})\mathbf{n_0} + \mathbf{z},$$

squaring this gives

$$\begin{aligned}|\boldsymbol{l}_0^{1/2}\mathbf{z}|^2 &= 1 + 2(\sqrt{r}-1)(\mathbf{n_0}\cdot\mathbf{z})^2 + (\sqrt{r}-1)^2(\mathbf{n_0}\cdot\mathbf{z})^2 \\ &= 1 + [2(\sqrt{r}-1)+(\sqrt{r}-1)^2]\cos^2\theta \\ &= 1 + (r-1)\cos^2\theta = \rho.\end{aligned}$$

Similarly,

$$\begin{aligned}\boldsymbol{l}_0\mathbf{z} &= (r-1)(\mathbf{n_0}\cdot\mathbf{z})\mathbf{n_0} + \mathbf{z} \\ &= (r-1)\cos(\theta)\sin(\theta)\mathbf{x} + [(r-1)\cos^2(\theta)+1]\mathbf{z} \\ &= -\alpha\mathbf{x} + \rho\mathbf{z}.\end{aligned}$$

Putting these results together, we get the required result,

$$\boldsymbol{l}_0^{1/2}\mathbf{b} = \frac{-\alpha}{\sqrt{\rho}}\mathbf{x} + \sqrt{\rho}\mathbf{z}.$$

1. Class 1: Reference state boundary normal $\mathbf{m}_1 \propto d\mathbf{b}+e\cos(b)\mathbf{x}'$

a. Recap

It was shown in Sec. V that if a sample in the reference state is split into two regions by a plane boundary with normal $\mathbf{m}_1 \propto d\mathbf{b}+e\cos(b)\mathbf{x}'$ then there is one (possibly b dependent) rotation $\mathbf{Q_1}$ such that if the deformations $\boldsymbol{\Lambda_1} = \mathbf{Q}_1\boldsymbol{l}_0^{1/2}\mathbf{B}_b$ and $\boldsymbol{\Lambda_2} = \boldsymbol{l}_0^{1/2}\mathbf{B}_{-b}$ are applied on either side of the boundary a the sample does not fracture. The deformations that make up the stripe domain satisfy the continuity equation

$$\boldsymbol{\Lambda}_1 - \boldsymbol{\Lambda}_2 = \mathbf{a}\otimes\mathbf{m}_1 \tag{A4}$$

for one (unknown and unimportant) vector $\mathbf{a}$.

b. Calculating $\mathbf{Q_1}$

Before the properties of the stripe domain can be addressed, $\mathbf{Q_1}$ must be calculated so that the deformations that give rise to the texture are fully specified. This is done by finding two constraints on $\mathbf{Q}_1$. First, if the stripe domain is to remain continuous under the deformations, the texture boundary must map to the same plane under both deformations. This means that the boundary normal in the final state $\mathbf{k}$ can be calculated as the transform of $\mathbf{m}_1$ under either deformation and both these ways of calculating $\mathbf{k}$ must agree

$$\mathbf{k} \propto \boldsymbol{\Lambda}_1^{-T}\mathbf{m}_1 \propto \boldsymbol{\Lambda}_2^{-T}\mathbf{m}_1.$$

Using $\boldsymbol{\Lambda_2}$,

$$\begin{aligned}\mathbf{k} &\propto \boldsymbol{\Lambda}_2^{-T}\mathbf{m}_1 \propto (\boldsymbol{l}_0^{1/2}\mathbf{B}_{-b})^{-T}\mathbf{m}_1 \\ &= \boldsymbol{l}_0^{-1/2}\{d\mathbf{b} + e\cos(b)[\cos(b)\mathbf{x}' + \sin(b)\mathbf{y}]\},\end{aligned}$$

giving

$$\begin{aligned}\mathbf{k} \propto &\left(\frac{\sqrt{r}\cos(\theta)}{\rho} + \frac{\alpha\sin(\theta)\cos^2(b)}{\sqrt{r\rho}}\right)\mathbf{z} + \sin(\theta)\cos(b) \\ &\times\left[\frac{\cos(b)\sqrt{\rho}}{\sqrt{r}}\mathbf{x} + \sin(b)\mathbf{y}\right].\end{aligned} \tag{A5}$$

Similarly, using $\boldsymbol{\Lambda_1}$,

$$\begin{aligned}\mathbf{k} \propto \mathbf{Q_1}\Bigg\{&\left(\frac{\sqrt{r}\cos(\theta)}{\rho} + \frac{\alpha\sin(\theta)\cos^2(b)}{\sqrt{r\rho}}\right)\mathbf{z} + \sin(\theta)\cos(b) \\ &\times\left[\frac{\cos(b)\sqrt{\rho}}{\sqrt{r}}\mathbf{x} - \sin(b)\mathbf{y}\right]\Bigg\}.\end{aligned}$$

This reveals that $\mathbf{Q_1}$ must be a rotation that reverses the y component of $\mathbf{k}$. This observation does not uniquely determine $\mathbf{Q}_1$ so another constraint is needed. This is found by postmultiplying continuity (A4) by $\mathbf{y}$, giving

$$\mathbf{Q}_1\boldsymbol{l}_0^{1/2}\mathbf{B}_b\mathbf{y} = \boldsymbol{l}_0^{1/2}\mathbf{B}_{-b}\mathbf{y}.$$

This shows that $\mathbf{Q}_1$ maps $\boldsymbol{l}_0^{1/2}\mathbf{B}_b\mathbf{y}$ onto $\boldsymbol{l}_0^{1/2}\mathbf{B}_{-b}\mathbf{y}$. Both these vectors lie in the x-y plane as the rotations about $\mathbf{b}$ ($\equiv\mathbf{z}'$) introduce an $\mathbf{x}'$ component to the $\mathbf{y}$ vector and the $\boldsymbol{l}_0^{1/2}$ operator does not change $\mathbf{y}$ but transforms $\mathbf{x}'$ into $\mathbf{x}$. Together with the requirement that $\mathbf{Q_1}$ reverses the $\mathbf{y}$ component of $\mathbf{k}$, this determines that the axis of $\mathbf{Q_1}$ is $\mathbf{z}$. If ϕ is the angle between the component of $\mathbf{k}$ in the x-y plane and the x axis, the angle of rotation is 2ϕ. Inspecting $\mathbf{k}$ gives

$$\tan^2\phi = \frac{r}{\rho}\tan^2(b).$$

c. Calculating the liquid-crystal directors

The director in the final state is different in the two regions. Let it be $\mathbf{n_1}$ in the $\boldsymbol{\Lambda}_1$ region and $\mathbf{n_2}$ in the $\boldsymbol{\Lambda}_2$ region. Calculating these directors is trivial; the director is not defined in the reference state (which has an isotropic step length tensor) but is introduced along $\mathbf{n}_0$ when the $\boldsymbol{l}_0^{1/2}$ component of the deformation is applied and transforms as a line element under the subsequent rotations. Therefore, $\mathbf{n_1} = \mathbf{Q}_1\mathbf{n}_0 = [\cos(2\phi)\mathbf{x} + \sin(2\phi)\mathbf{y}]\sin(\theta) + \cos(\theta)\mathbf{z}$ and $\mathbf{n_2} = \mathbf{n}_0 = \mathbf{x}\sin(\theta) + \cos(\theta)\mathbf{z}$. This means that ϕ is (half) the angle between the components of the LC director in the LC plane

in the two regions and as such is a physically meaningful variable that could be measured in the final state.

d. Calculating the liquid-crystal layer normals

In both regions, the LC layer normals are aligned with the $\mathbf{z}$ axis. This is shown by starting with $\mathbf{b}$, the layer normal in the reference state, and following how it transforms under the deformations, for example, in the $\mathbf{\Lambda_1}$ region

$$(\mathbf{Q}_1\boldsymbol{l}_0^{1/2}\mathbf{B}_b)^{-T}\mathbf{b} = \mathbf{Q}_1\boldsymbol{l}_0^{-1/2}\mathbf{B}_b\mathbf{b} = \mathbf{Q}_1\boldsymbol{l}_0^{-1/2}\mathbf{b} = \mathbf{Q_1 z} = \mathbf{z}.$$

The proof in the second region is almost identical but without the $\mathbf{Q}_1$.

e. Description of the stripe domains

Having found the final-state directors, layer normals, and boundary normal, the stripe-domains are in principle completely described. However, the above results can be brought together with one simple relation. Let χ be the angle between the boundary plane and the layer plane (which is still the x-y plane). The tangent of this angle can be calculated by inspecting $\mathbf{k}$ in Eq. (A5),

$$\tan(\chi) = \frac{\sin(\theta)\cos(b)\sqrt{\frac{\cos^2(b)\rho}{r} + \sin^2(b)}}{\sqrt{\frac{r}{\rho}}\cos(\theta) - \frac{r-1}{\sqrt{r\rho}}\sin^2(\theta)\cos^2(b)\cos(\theta)},$$

which simplifies to

$$\tan(\chi) = \tan(\theta)\cos(\phi).$$

This result mirrors its equivalent in the second class of stripe domains better if ϕ is replaced by $\gamma = \pi/2 - \phi$. Physically, γ is the angle between the component of the LC rods in the layer plane and the texture boundary measured through the layer plane. Substituting for γ gives

$$\tan(\chi) = \tan(\theta)\sin(\gamma).$$

This describes fully the boundary and director properties of this type of stripe domain. The structure of the texture is illustrated in Fig. 2.

The soft textures described by Adams and Warner in [5] are built out of this type. To bring these descriptions into the Adams and Warner form, the whole sample must be rotated about the z axis by ϕ after deformation which eliminates the y component of the texture normal $\mathbf{k}$.

2. Class 2: Reference state boundary normal $\mathbf{m}_2 = \mathbf{y}$

a. Recap

It was shown in Sec. V that if a sample in the reference state is split into two regions by a plane boundary with normal $\mathbf{m}_2 = \mathbf{y}$ then there is one (possibly b dependent) rotation $\mathbf{Q_2}$ such that if the deformations $\mathbf{\Lambda_1'} = \mathbf{Q}_2\boldsymbol{l}_0^{1/2}\mathbf{B}_b$ and $\mathbf{\Lambda_2'} = \boldsymbol{l}_0^{1/2}\mathbf{B}_{-b}$ are applied on either side of the boundary, the material does not fracture.

The interface satisfies the continuity equation

$$\mathbf{\Lambda}_1' - \mathbf{\Lambda}_2' = \mathbf{a}' \otimes \mathbf{m}_2 \tag{A6}$$

for one (unknown and unimportant) vector $\mathbf{a}'$.

b. Rotation of the sample after deformation

Rotating the whole sample after deformation does not change any of the intrinsic properties of the stripe domain or $\mathbf{m}_2$ (which is defined in the reference state). The calculations that follow are significantly simplified if the entire sample is rotated by $\mathbf{Q}_2^{-1/2}$ after the other deformations as the vectors we are trying to calculate (such as the layer normal) align better with the axes. This additional rotation is incorporated into our notation by defining the deformation in one region as $\mathbf{\Lambda_1} = \mathbf{Q}_2^{1/2}\boldsymbol{l}_0^{1/2}\mathbf{B}_b$ and that in the other as $\mathbf{\Lambda_2} = \mathbf{Q}_2^{-1/2}\boldsymbol{l}_0^{1/2}\mathbf{B}_{-b}$.

The continuity equation now reads as

$$\mathbf{\Lambda}_1 - \mathbf{\Lambda}_2 = \mathbf{a} \otimes \mathbf{m}_2 \tag{A7}$$

where $\mathbf{a} = \mathbf{Q}_2^{-1/2}\mathbf{a}'$.

c. Calculating $\mathbf{Q_2}$

This calculation proceeds in a manner completely analogous to the (more detailed) calculation in Appendix A, Sec. 1b.

Let $\mathbf{k}$ be the final-state boundary normal. Calculating it using $\mathbf{\Lambda_2}$ gives

$$\mathbf{k} \propto (\mathbf{Q}_2^{-1/2}\boldsymbol{l}_0^{1/2}\mathbf{B}_{-b})^{-T}\mathbf{m}_2 = \mathbf{Q}_2^{-1/2}\boldsymbol{l}_0^{-1/2}\mathbf{B}_{-b}\mathbf{y},$$

$$\mathbf{k} \propto \mathbf{Q}_2^{-1/2}\left[\mathbf{y}\cos(b) - \sqrt{\frac{\rho}{r}}\sin(b)\mathbf{x} - \frac{\alpha}{\sqrt{\rho r}}\sin(b)\mathbf{z}\right].$$

Similarly, using $\mathbf{\Lambda_1}$ gives

$$\mathbf{k} \propto (\mathbf{Q}_2^{1/2}\boldsymbol{l}_0^{1/2}\mathbf{B}_b)^{-T}\mathbf{m}_2 = \mathbf{Q}_2^{1/2}\left[\mathbf{y}\cos(b) + \sqrt{\frac{\rho}{r}}\sin(b)\mathbf{x} + \frac{\alpha}{\sqrt{\rho r}}\sin(b)\mathbf{z}\right].$$

Since both these ways of calculating $\mathbf{k}$ must give the same answer, this places one constraint on $\mathbf{Q}_2$. As in the first case, this does not uniquely identify $\mathbf{Q}_2$; but a second constraint can be found be multiplying the continuity equation by $\mathbf{b}$, giving

$$\mathbf{Q}_2\boldsymbol{l}_0^{1/2}\mathbf{B}_b\mathbf{b} = \boldsymbol{l}_0^{1/2}\mathbf{B}_{-b}\mathbf{b},$$

$$\mathbf{Q}_2\boldsymbol{l}_0^{1/2}\mathbf{b} = \boldsymbol{l}_0^{1/2}\mathbf{b}.$$

This implies that the axis of $\mathbf{Q}_2$ is $\boldsymbol{l}_0^{1/2}\mathbf{b}$. Since

$$\boldsymbol{l}_0^{1/2}\mathbf{b} = \frac{-\alpha}{\sqrt{\rho}}\mathbf{x} + \sqrt{\rho}\mathbf{z}$$

is perpendicular to both $\mathbf{Q}_2^{-1/2}\mathbf{k}$ and $\mathbf{Q}_2^{1/2}\mathbf{k}$ and $\mathbf{Q}_2$ maps between these vectors, the angle of rotation can be found from the dot product of these two vectors. Defining the angle as 2ϕ (so that angle of $\mathbf{Q}_2^{1/2}$ is ϕ),

$$\cos(2\phi) = \frac{\cos^2(b) - \sin^2(b)\left(\frac{\rho}{r} + \frac{\alpha^2}{\rho r}\right)}{\cos^2(b) + \sin^2(b)\left(\frac{\rho}{r} + \frac{\alpha^2}{\rho r}\right)},$$

which simplifies to

$$\tan^2(\phi) = \left(\frac{\rho}{r} + \frac{\alpha^2}{\rho r}\right)\tan^2(b).$$

The observation that the axis of $\mathbf{Q}_2$ is perpendicular to both $\mathbf{Q}_2^{-1/2}\mathbf{k}$ and $\mathbf{Q}_2^{1/2}\mathbf{k}$ determines that

$$\mathbf{k} = \mathbf{y}.$$

d. Calculating the liquid-crystal layer normals

The next step is to calculate the LC layer normals in each region $\mathbf{d}_+$ (in the first region) and $\mathbf{d}_-$ (in the second region). As before, this is done by transforming $\mathbf{b}$ with the deformation tensor in each region, giving

$$\mathbf{d}_\pm = (\mathbf{Q}_2^{\pm 1/2}\boldsymbol{l}_0^{1/2}\mathbf{B}_{\pm b})^{-T}\mathbf{b} = \mathbf{Q}_2^{\pm 1/2}\mathbf{z}.$$

Calculating these vectors explicitly is straightforward but tedious. One must construct an orthonormal set of vectors: one along the axis of $\mathbf{Q}$, one in the direction of the component of $\mathbf{z}$ perpendicular to the axis, and one along the cross product of these two directions. After decomposing $\mathbf{z}$ into this basis, the rotation is easy to implement. The result of the calculation is

$$\mathbf{d}_\pm = \frac{\alpha}{\beta}\left\{\rho[1-\cos(\phi)]\mathbf{x} \pm \sqrt{\beta}\sin(\phi)\mathbf{y} - \left[\frac{\rho^2}{\alpha} + \alpha\cos(\phi)\right]\mathbf{z}\right\}.$$

As the two layer normals are not equal, the LC layers are bent at the texture boundary. The angle between the LC layer plane and the boundary plane χ (which is the same in both regions) can be found by taking the dot product of $\mathbf{d}_\pm$ and $\mathbf{y}$, giving,

$$\cos(\chi) = \frac{\alpha}{\sqrt{\beta}}\sin(\phi).$$

e. Calculating the liquid-crystal directors

Further characterization of the solutions requires calculation of the LC directors in the final state. The component of the director along the LC layer normal transforms with the layer normal, so only the component in the layer needs to be calculated. As in case one, it is not defined in the reference state (which has an isotropic step length tensor) but is introduced into the system along $\mathbf{x}$ when the $\boldsymbol{l}_0^{1/2}$ deformation is imposed (which returns a relaxed Sm-C state with a director) and transforms as a line element under the subsequent rotations. If the component of the LC director in the LC layer plane is defined as $\mathbf{c}_+$ in the first region and $\mathbf{c}_-$ in the second region,

$$\mathbf{c}_\pm = \mathbf{Q}_2^{\pm 1/2}\mathbf{x}.$$

This can be evaluated in the same manner as $\mathbf{Q}_2^{\pm 1/2}\mathbf{z}$ above yielding,

$$\mathbf{c}_\pm = \frac{\rho}{\beta}\left\{\left[\frac{\alpha^2}{\rho} + \rho\cos(\phi)\right]\mathbf{x} \pm \sqrt{\beta}\sin\phi\mathbf{y} + \alpha[\cos(\phi)-1]\mathbf{z}\right\}.$$

f. Describing the stripe domain

As in the first case, the above results can be brought together into one relation if γ is the angle between the component of the LC director in the LC layer and the boundary plane, measured through the LC layer then

$$\sin(\gamma) = \frac{\rho}{\alpha}\cot(\chi).$$

This is an important result as it links two quantities (γ and χ) that can be measured in the final state. The straightforward (but algebraically tedious) proof of this result is given in Appendix B.

The structure of this stripe domain is shown diagrammatically in Fig. 3.

3. Shear angle

The shear angle for both categories of stripe domain is given by Eq. (6.3). Since it is the same for both categories, we can choose whether to use the type-1 or type-2 boundary normal. Here we use the type-2 boundary, $\mathbf{m}=\mathbf{y}$ so,

$$\begin{aligned}\boldsymbol{\Lambda}_2\mathbf{m} &= \boldsymbol{l}_0^{1/2}\mathbf{B}_{-b}\mathbf{y}\\ &= \boldsymbol{l}_0^{1/2}[\cos(b)\mathbf{y} - \sin(b)\mathbf{x}']\\ &= \cos(b)\mathbf{y} + \sin(b)\sqrt{\frac{r}{\rho}}\mathbf{x},\end{aligned}$$

and similarly,

$$\begin{aligned}\boldsymbol{\Lambda}_2^{-T}\mathbf{m} &= \boldsymbol{l}_0^{-1/2}\mathbf{B}_{-b}\mathbf{y}\\ &= \boldsymbol{l}_0^{-1/2}[\cos(b)\mathbf{y} - \sin(b)\mathbf{x}']\\ &= \cos(b)\mathbf{y} + \sin(b)\left(\sqrt{\frac{\rho}{r}}\mathbf{x} + \frac{\alpha}{\sqrt{\rho r}}\mathbf{z}\right).\end{aligned}$$

Putting these two results into Eq. (6.3), the shear angle is

$$\frac{1}{2}\tan(\zeta) = \sqrt{\left[\cos^2(b) + \frac{r}{\rho}\sin^2(b)\right]\left[\cos^2(b) + \left(\frac{\rho}{r} + \frac{\alpha^2}{\rho r}\right)\sin^2(b)\right] - 1}. \quad \text{(A8)}$$

APPENDIX B: DERIVATION OF $\sin(\gamma)=\frac{\rho}{\alpha}\cot(\chi)$

To calculate γ we need to calculate a vector in both the layer and texture planes ($\mathbf{g}$). This can be done by taking the cross product of the layer normals on each side of the interface and normalizing the result to a unit vector. This procedure gives

$$\mathbf{g}=\frac{\left\{\left[\frac{-\rho^2}{\alpha}-\alpha\cos(\phi)\right]\mathbf{x}-\rho[1-\cos(\phi)]\mathbf{z}\right\}}{\sqrt{\beta\left[\frac{\rho^2}{\alpha^2}+\cos^2(\phi)\right]}}.$$

Since γ is the angle between $\mathbf{g}$ and $\mathbf{c}_{\pm}$, it can be found by taking their dot product. The following two rearrangements significantly simplify the resulting expressions.

First, using $\rho^2+\alpha^2=\beta$,

$$\frac{\rho^2}{\alpha^2}+\cos^2(\phi)=\frac{\beta}{\alpha^2}-1+\cos^2(\phi),$$

and using $\cos(\chi)=\frac{\alpha}{\sqrt{\beta}}\sin(\phi)$,

$$\frac{\beta}{\alpha^2}-1+\cos^2(\phi)=\frac{\beta}{\alpha^2}\left[1-\frac{\alpha^2}{\beta}\sin^2(\phi)\right]=\frac{\beta}{\alpha^2}\sin^2(\chi).$$

Second, multiplying out,

$$\left[\frac{\alpha^2}{\rho}+\rho\cos(\phi)\right]\left[\frac{\rho^2}{\alpha}+\alpha\cos(\phi)\right]-\rho\alpha[1-\cos(\phi)]^2, \tag{B1}$$

$$=\rho\alpha\left(\frac{\alpha^2}{\rho^2}+\frac{\rho^2}{\alpha^2}+2\right)\cos(\phi), \tag{B2}$$

and using $\rho^2+\alpha^2=\beta$,

$$\rho\alpha\left(\frac{\alpha^2}{\rho^2}+\frac{\rho^2}{\alpha^2}+2\right)\cos(\phi)=\frac{\beta^2}{\rho\alpha}\cos(\phi).$$

Armed with these rearrangements, the dot product immediately simplifies to

$$\cos(\gamma)=\frac{\cos(\phi)}{\sin(\chi)}.$$

Using $\cos(\chi)=\frac{\alpha}{\sqrt{\beta}}\sin(\phi)$ to substitute for ϕ and pythagoras to turn the $\cos(\gamma)$ into a $\sin(\gamma)$ gives

$$\sin(\gamma)=\sqrt{1-\frac{1-\frac{\beta}{\alpha^2}\cos^2(\chi)}{\sin^2(\chi)}}, \tag{B3}$$

$$=\sqrt{\left(1-\frac{\beta}{\alpha^2}\right)\left(1-\frac{1}{\sin^2(\chi)}\right)}, \tag{B4}$$

$$=\sqrt{\left(1-\frac{\beta}{\alpha^2}\right)}\cot(\chi). \tag{B5}$$

Finally, using once again $\rho^2+\alpha^2=\beta$,

$$\sin(\gamma)=\frac{\rho}{\alpha}\cot(\chi)$$

which is the desired result.

APPENDIX C: CONSEQUENCES OF BIAXIALITY

A more refined model for Sm-C elastomers could be constructed by replacing $\boldsymbol{l}_0$ by a biaxial tensor $\boldsymbol{T}_0$. Since this tensor defines the spontaneous distortion from the reference state to the relaxed state, we require it to be symmetric and have a determinant of one. A Sm-C phase is defined by two "double headed" vectors, the rod director, which we call here $\mathbf{n}_0'$, and the layer normal $\mathbf{z}$. Therefore, $\boldsymbol{T}_0$ must be constructed using symmetric and even combinations of these vectors, the identity $\boldsymbol{I}$ and, in the Sm-C^* case, the Levi-Civita tensor $\boldsymbol{\epsilon}_{ijk}$. By considering all admissible combinations, it is clear that $\boldsymbol{T}_0$ must have one principal direction perpendicular to both $\mathbf{n}_0'$ and $\mathbf{z}$—that is along $\mathbf{y}$—and that the other two must lie in the $\mathbf{n}_0'$-$\mathbf{z}$ plane. We call these two directions $\mathbf{n}_0$ and $\mathbf{v}$, so that

$$\boldsymbol{T}_0=a\mathbf{n}_0\otimes\mathbf{n}_0+b\mathbf{y}\otimes\mathbf{y}+\frac{1}{ab}\mathbf{v}\otimes\mathbf{v}. \tag{C1}$$

We expect biaxiality to be fairly small so that this tensor still resembles the original $\boldsymbol{l}_0$, meaning that the principal direction $\mathbf{n}_0$, associated with the largest principal value of $\boldsymbol{T}_0$, will be close to the rod director $\mathbf{n}_0'$. The new set of soft modes is simply anything that can be written in the form

$$\boldsymbol{\Lambda}=\mathbf{Q}_1\boldsymbol{T}_0^{1/2}\mathbf{B}, \tag{C2}$$

where, as in Eq. (3.4), $\boldsymbol{Q}_1$ is any rotation and $\boldsymbol{B}$ is any rotation about $\mathbf{b}$. Repeating the arguments of Sec. V for this set of deformations, we see that we can, without loss of generality, limit attention to stripe domains between two deformations of the forms $\mathbf{Q}\mathbf{T}_0^{1/2}\mathbf{B}_b$ and $\mathbf{T}_0^{1/2}\mathbf{B}_{-b}$. Continuing to follow Sec. V, Mallard's law will be satisfied if there is a rotation $\boldsymbol{Q}_3$ and a π rotation $\boldsymbol{R}$ such that

$$\boldsymbol{T}_0^{1/2}\boldsymbol{B}_b=\boldsymbol{Q}_3\boldsymbol{T}_0^{1/2}\boldsymbol{B}_{-b}\boldsymbol{R}, \tag{C3}$$

which is the analog of Eq. (5.8). As in the uniaxial case, the choice $\boldsymbol{R}=\boldsymbol{Q}_3=\boldsymbol{R}_\mathbf{y}$, where $\boldsymbol{R}_\mathbf{y}$ is a π rotation about $\mathbf{y}$, satisfies this equation since $\mathbf{y}$ is perpendicular to $\mathbf{b}$, $\mathbf{n}_0$, and $\mathbf{v}$ so $\mathbf{B}_{-b}\mathbf{R}_\mathbf{y}=\mathbf{R}_\mathbf{y}\mathbf{B}_b$ and $\mathbf{R}_\mathbf{y}\boldsymbol{T}_0^{1/2}\mathbf{R}_\mathbf{y}=\boldsymbol{T}_0^{1/2}$.

Unlike in the uniaxial case, there is not another choice of $\boldsymbol{R}$ and $\boldsymbol{Q}_3$ that also satisfies Mallard's law; but both categories of solution still exist as the two types of solutions generated by the one possibility for $\boldsymbol{R}$ [Eqs. (5.4) and (5.5)]. Furthermore, since the conditions in Sec. VII are satisfied by the $\boldsymbol{R}=\boldsymbol{R}_\mathbf{y}$ solutions, the structure of one charged class and one uncharged class is also unchanged. Finally, the property that the layer normals are the same on either side of the interface in the charged class of stripe domains also survives the addition of biaxiality. The layer normal after the imposition of a deformation $\boldsymbol{Q}\boldsymbol{T}_0^{1/2}\boldsymbol{B}$ will be $\boldsymbol{Q}\boldsymbol{T}_0^{-1/2}\mathbf{b}$. Taking two representative deformations, the continuity equation gives

$$\boldsymbol{Q}\boldsymbol{T}_0^{1/2}\boldsymbol{B}_b-\boldsymbol{T}_0^{1/2}\boldsymbol{B}_{-b}=\mathbf{a}\otimes\mathbf{m}, \tag{C4}$$

and the two final-state layer normals will be $\boldsymbol{Q}\boldsymbol{T}_0^{-1/2}\mathbf{b}$ and $\boldsymbol{T}_0^{-1/2}\mathbf{b}$, respectively. Calculating the two Mallard's law solutions to this equation generated by $\boldsymbol{R}=\boldsymbol{R}_\mathbf{y}$, we see that the second solution [Eq. (5.5)] has the property that

$\mathbf{a} \propto \boldsymbol{T}_0^{1/2}\boldsymbol{B}_{-b}\mathbf{y}$. This is perpendicular to $\boldsymbol{T}_0^{-1/2}\mathbf{b}$, so contracting the continuity equation with $\boldsymbol{T}_0^{-1/2}\mathbf{b}$ from the left gives

$$\mathbf{b}\boldsymbol{T}_0^{-1/2}\boldsymbol{Q}\boldsymbol{T}_0^{1/2}\boldsymbol{B}_b = \mathbf{b}\boldsymbol{T}_0^{-1/2}\boldsymbol{T}_0^{1/2}\boldsymbol{B}_{-b}, \tag{C5}$$

which simplifies to

$$\boldsymbol{Q}\boldsymbol{T}_0^{-1/2}\mathbf{b} = \boldsymbol{T}_0^{-1/2}\boldsymbol{B}_{-b}\mathbf{b}, \tag{C6}$$

which are the two final-state layer normals; so for this class of twins the two final-state layer normals are parallel even with the addition of biaxiality. This means that all the qualitative structure of the stripe domains is unaffected by the addition of biaxiality, although we expect that the precise relations between the various angles will be.

[1] M. Warner and E. M. Terentjev, *Liquid Crystal Elastomers* (Oxford University Press, New York, 2003); *Liquid Crystal Elastomers*, paperback edition (Oxford University Press, New York, 2007).

[2] M. Warner, P. Bladon, and E. M. Terentjev, J. Phys. II **4**, 93 (1994).

[3] J. M. Adams and M. Warner, Phys. Rev. E **72**, 011703 (2005).

[4] H. Finkelmann, I. M. Kundler, E. M. Terentjev, and M. Warner, J. Phys. II **7**, 1059 (1997).

[5] J. M. Adams and M. Warner, Phys. Rev. E **79**, 061704 (2009).

[6] J. M. Adams, S. Conti, and A. DeSimone, J. Cont. Mech. Ther. **18**, 319 (2006).

[7] K. Bhattacharya, *Microstructure of Martensite* (Oxford University Press, New York, 2003).

[8] P. D. Olmsted, J. Phys. II **4**, 2215 (1994).

[9] J. M. Ball and R. D. James, Arch. Ration. Mech. Anal. **100**, 13 (1987).

[10] J. L. Ericksen, J. Therm. Streses **4**, 107 (1981).